Journal of Medicinal Chemistry

Article

pubs.acs.org/jmc

Synthesis, Biological Evaluation, and Molecular Modeling of Glycyrrhizin Derivatives as Potent High-Mobility Group Box-1 Inhibitors with Anti-Heart-Failure Activity in Vivo

Dan Du,[†] Jun Yan,[†] Jinhong Ren,[†] Haining Lv, Yong Li, Song Xu, Yadan Wang, Shuanggang Ma, Jing Qu, Weibin Tang, Zhuowei Hu,* and Shishan Yu*

State Key Laboratory of Bioactive Substance and Function of Natural Medicines, Institute of Materia Medica, Chinese Academy of Medical Sciences and Peking Union Medical College, Beijing 100050, China

Supporting Information

ABSTRACT: Novel glycyrrhizin (GL) derivatives were designed and synthesized by introducing various amine or amino acid residues into the carbohydrate chain and at C-30. Their inhibitory effects on high-mobility group box 1 (HMGB1) were evaluated using a cell-based lipopolysaccharide (LPS) induced tumor necrosis factor α (TNF-α) release study. Compounds **10**, **12**, **18**−**20**, **23**, and **24**, which had substituents introduced at C-30, demonstrated moderate HMGB1 inhibition with ED_{50} values ranging from 337 to 141 μM, which are values comparable to that of the leading GL compound (**1**) (ED_{50} = 70 μM). Compounds **23** and **24** emerged as novel and interesting HMGB1 inhibitors. These compounds were able to extend the survival of mice with chronic heart failure (CHF) and acute heart failure (AHF), respectively. In addition, molecular modeling studies were performed to support the biological data.

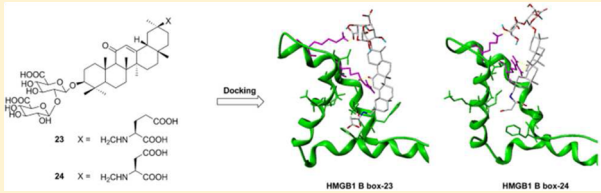

INTRODUCTION

Heart failure (HF) is a serious public health problem that is characterized by the inability of the heart to sufficiently distribute blood to meet the needs of the body.[1] Common causes of HF include myocardial infarction and other forms of ischemic heart disease, hypertension, valvular heart disease, and cardiomyopathy.[2] Echocardiography is commonly used to support the clinical diagnosis of HF. This modality uses ultrasound to determine the stroke volume, end diastolic volume, and ejection fraction. Chronic heart failure (CHF) represents a long-term condition that usually shows stabilized symptomatology. Acute heart failure (AHF) refers to episodes in which a patient displays a change in heart failure signs and symptoms, resulting in a need for urgent therapy or hospitalization.[3] Although various agents, devices, and surgical treatments are currently used for HF, few are ideal for the treatment of its associated pathologies. HF is a common, costly, disabling, and potentially deadly condition.[2] Postmyocardial infarction remodeling, morbidity, and mortality are highly dependent on the number of cardiomyocytes lost during ischemic injury. However, emerging data now provide convincing evidence that the heart possesses a regenerative capacity from both endogenous and exogenous sources.[4,5] Inflammation, which has emerged as a critical biological process that contributes to nearly all aspects of cardiovascular diseases including HF, plays a paradoxical role in cardiac repair and regeneration. An array of cytokines has been implicated in the activation of the inflammatory response as well as in the healing and repair process.[4]

High-mobility group box 1 protein (HMGB1) is localized in the nucleus and can be either passively released from necrotic cells or actively secreted by activated macrophages/monocytes to serve as an extracellular signaling molecule involved in acute and chronic inflammation.[6] The investigation of HMGB1 as a regenerative and proliferative agent in the myocardium was first suggested by Roberta et al.[7,8] HMGB1 has been reported to stimulate angiogenesis and promote cardiac stem cell growth and differentiation.[9−11] Notably, several HMGB1-inhibiting agents (e.g., ethyl pyruvate, green tea, and adrenomedullin) can preserve cardiac function after myocardial ischemia, which is consistent with the pathogenic role of HMGB1 in cardiovascular diseases.[12] HMGB1 has three major structural domains: two DNA binding motifs, called the A box and B box, and an acidic carboxyl terminus. It has been revealed that the proinflammatory activity of HMGB1 localizes to the B box with the most significant cytokine functionality mapping to the first 20 amino acid residues of this domain (HMGB1 amino acids 89−108).[13] The A box exerts an antagonistic, anti-inflammatory effect, perhaps by binding unproductively to glycation end products (RAGE) and competing with functional HMGB1.[10−12] Hence, the appropriate inhibition of HMGB1 by targeted binding to the B box has arisen as an efficient therapeutic strategy for cardiovascular diseases.[13,16,17]

Natural products play a major role in drug discovery, and nearly half of the new drugs introduced into the market over

Received: August 29, 2012
Published: November 30, 2012

Scheme 1. Synthesis of Glycyrrhizin Intermediates 2−4[a]

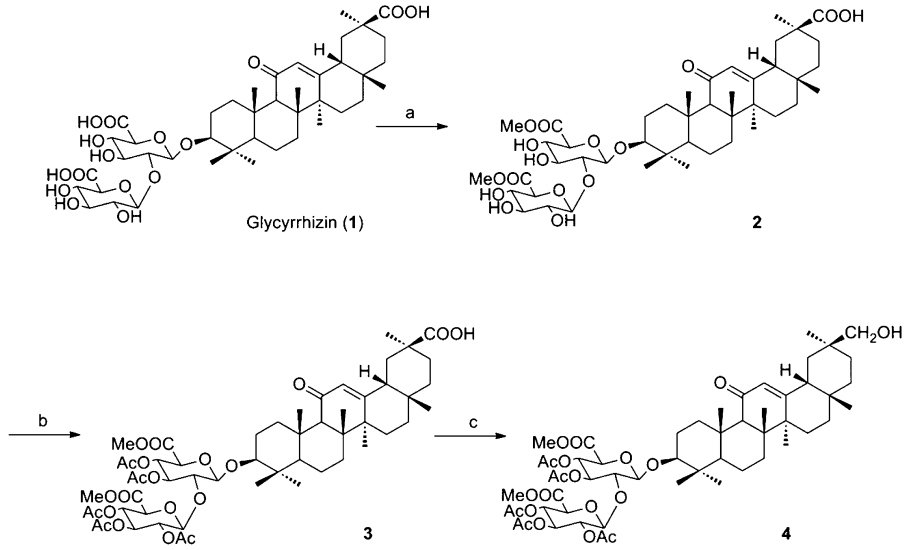

[a](a) 2% methanolic HCl, rt, 2h, Et_3N, 90%; (b) $Ac_2O-C_5H_5N$, rt, 4h, 72%; (c) (i) $ClCOOC_2H_5$, Et_3N, THF, −5 °C, 30 min; (ii) $NaBH_4$, H_2O, rt, 4h, two steps 58%.

Scheme 2. Synthesis of Glycyrrhizin Derivatives 5−8[a]

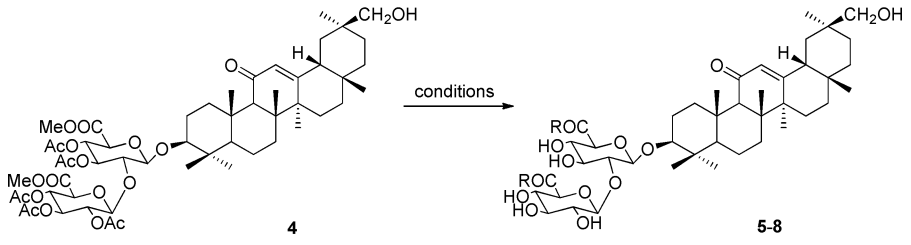

compound	R	conditions
5		a
6	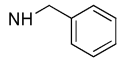	b
7		c
8	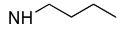	d

[a](a) Propylamine, sealed tube, 80 °C, 4 h, 47%; (b) benzylamine, sealed tube, 80 °C, 4 h, 65%; (c) ethanolamine, sealed tube, 80 °C, 4 h, 49%; (d) butylamine, sealed tube, 80 °C, 4 h, 47%.

the past 2 decades are natural products or their derivatives.[18] GL (**1**) is the major bioactive triterpene glycoside of licorice root extract and possesses a wide range of pharmacological properties, especially anti-inflammatory properties. In a recent study by Mollica et al., GL was found to inhibit HMGB1 by directly binding (KD ≈ 150 μM) to each of the two HMG boxes and thus prohibiting its chemoattractant and mitogenic activities. Furthermore, the moiety of GL that is responsible for this binding is its triterpene ring, and a molecular model of the HMGB1−GL interaction has been created.[19] In Japan, Sitia et al. reported that treatment with GL as a HMGB1 inhibitor diminishes cytotoxic T lymphocyte induced liver disease in hepatitis B virus (HBV) transgenic mice.[20] Recently, we also found that GL can be used at low concentrations to treat heart failure by inhibiting HMGB1 (Supporting Information). Although excessive HMGB1 may play a pathogenic role in cardiovascular diseases, low levels of HMGB1 might be beneficial. To the best of our knowledge, the anti-HF activity of GL in vivo has not been investigated to date. It is thus important to pharmacologically attenuate (but not completely abrogate) HMGB1 release to interfere with the progression of various cardiovascular diseases and to facilitate the recovery of cardiovascular functions. Therefore, this profile prompted us to synthesize and evaluate derivatives related to GL to explore the structural requirements for the appropriate inhibition and selective binding of the B box.

To identify more potent HMGB1 inhibitors with increased water solubility, we designed and synthesized a series of GL derivatives by introducing amino acids into the carbohydrate chain and at C-30, and their biological activities are described in

dx.doi.org/10.1021/jm301248y | J. Med. Chem. 2013, 56, 97−108

Scheme 3. Synthesis of Glycyrrhizin Derivatives 9−24[a]

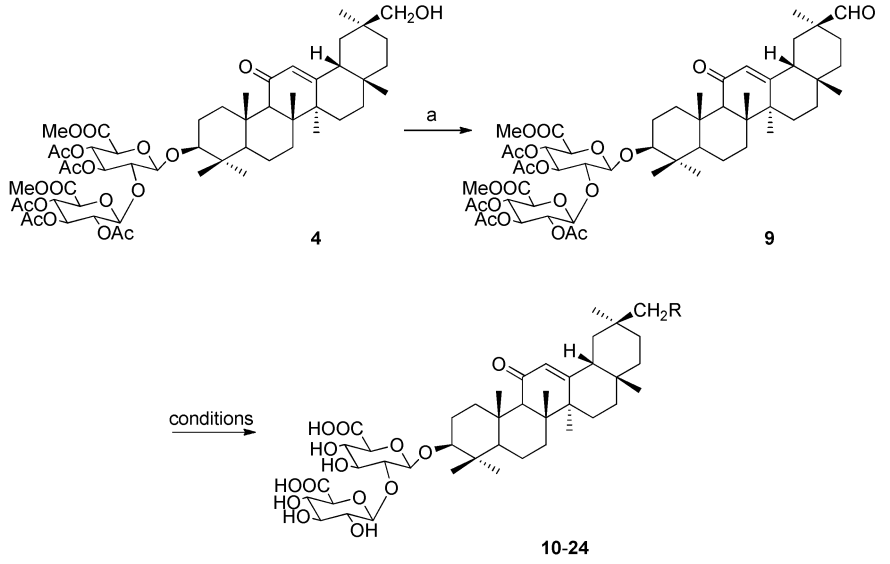

compound	R	conditions	compound	R	conditions
10	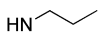	b	17	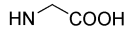	i
11		c	18	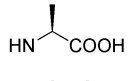	j
12	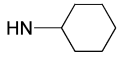	d	19	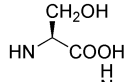	k
13	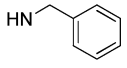	e	20	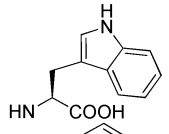	l
14	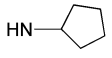	f	21	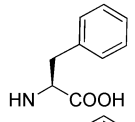	m
15	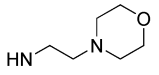	g	22	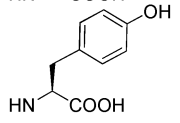	n
16	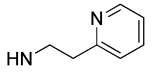	h	23	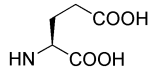	o
			24	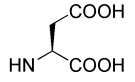	p

[a](a) PCC, CH_2Cl_2, 0 °C, rt, 2 h, 73%; (b) (i) $NaBH_3CN$, propylamine, MeOH, rt, 3 h, 53%; (ii) 5% KOH, EtOH/H_2O = 1:1, Amberlite 120 H^+ resin, 91%; (c) (i) $NaBH_3CN$, isopropylamine, rt, 3 h, 35%; (ii) 5% KOH, EtOH/H_2O = 1:1, Amberlite 120 H^+ resin, 89%; (d) (i) $NaBH_3CN$, cyclohexylamine, rt, 3 h, 48%; (ii) 5% KOH, EtOH/H_2O = 1:1, Amberlite 120 H^+ resin, 94%; (e) (i) $NaBH_3CN$, benzylamine, rt, 3 h, 61%; (ii) 5% KOH, EtOH/H_2O = 1:1, Amberlite 120 H^+ resin, 87%; (f) (i) $NaBH_3CN$, cyclopentylamine, rt, 3 h, 38%; (ii) 5% KOH, EtOH/H_2O = 1:1, Amberlite 120 H^+ resin, 98%; (g) (i) $NaBH_3CN$, 4-(2-aminoethyl) morpholine, rt, 3 h, 47.3%; (ii) 5% KOH, EtOH/H_2O = 1:1, Amberlite 120 H^+ resin, 91%; (h) (i) $NaBH_3CN$, 2-pyridylethylamine, rt, 3 h, 38%; (ii) 5% KOH, EtOH/H_2O = 1:1, Amberlite 120 H^+ resin, 83%; (i) (i) $NaBH_3CN$, L-Gly-OEt-HCl, MeOH, rt, 3 h, 62%; (ii) 5% KOH, EtOH/H_2O = 1:1, Amberlite 120 H^+ resin, 96%; (j) (i) $NaBH_3CN$, L-Ala-OMe-HCl, MeOH, rt, 3 h, 45%; (ii) 5% KOH, EtOH/H_2O = 1:1, Amberlite 120 H^+ resin, 94%; (k) (i) $NaBH_3CN$, L-Ser-OMe-HCl, MeOH, rt, 3 h, 49%; (ii) 5% KOH, EtOH/H_2O = 1:1, Amberlite 120 H^+ resin, 86%; (l) (i) $NaBH_3CN$, L-Try-OMe-HCl, MeOH, rt, 3 h, 59%; (ii) 5% KOH, EtOH/H_2O =1:1, Amberlite 120 H^+ resin, 94%; (m) (i) $NaBH_3CN$, L-Phe-OMe-HCl, MeOH, rt, 3 h, 66%; (ii) 5% KOH, EtOH/H_2O = 1:1, Amberlite 120 H^+ resin, 96%; (n) (i)$NaBH_3CN$, L-Tyr-OMe-HCl, MeOH, rt, 3 h, 37%; (ii) 5% KOH, EtOH/H_2O = 1:1, Amberlite 120 H^+ resin, 89%; (o) (i) (i) $NaBH_3CN$, L-Glu-$(OMe)_2$-HCl, MeOH, rt, 3 h, 48%; (ii) 5% KOH, EtOH/H_2O = 1:1, Amberlite 120 H^+ resin, 97%; (p) (i) $NaBH_3CN$, L-Asp-$(OMe)_2$-HCl, MeOH, rt, 3 h, 44%; (ii) 5% KOH, EtOH/H_2O = 1:1, Amberlite 120 H^+ resin, 96%.

this report. The inhibition of LPS-induced TNF-α secretion in RAW264.7 cells by these GL derivatives was tested in vitro. The results obtained demonstrated that compounds **23** and **24** were potent inhibitors of HMGB1. The anti-HF effects of the

dx.doi.org/10.1021/jm301248y | J. Med. Chem. 2013, 56, 97−108

promising GL derivatives were also evaluated based on their protective effects on cardiac dysfunctions and survival in doxorubicin (DOX) induced acute and chronic Doll Capital Management (DCM) mice in vivo.

RESULTS AND DISCUSSION

Chemistry. The series was designed based on the improved binding properties between GL and HMGB1 reported by Mollica et al.[19] as well as the chemical modifications of GL reviewed by Baltina.[21] In Mollica's study, the triterpene establishes favorable van der Waals interactions with the HMG boxes; the C-11 carbonyl group and C-30 carboxyl group of GL create a hydrogen bond or an electrostatic interaction with the amino acid group of the HMG boxes, and the sugar moieties point away from the protein. According to Baltina's review, elongation of the GL carbohydrate chains or introduction of amino acids or heterocyclic fragments has previously been shown to significantly affect the anti-inflammatory activities of glycosides. Because the carbonyl at C-11 is an inert site that is sterically hindered, it is not suitable for derivatization. In this regard, we chose to investigate whether chemical modifications of the carbohydrate chain and the C-30 carboxyl group affect the HMGB1 inhibitory activity. Consequently, amides **5**−**8** were synthesized and compounds **10**−**25** contain an amine or amino acid residue with a C−N bond through the amino group and C-30.

Compound **4**, the key intermediate for the synthesis of the target compounds (Scheme 1), was produced by treating the pentaacetate of the GL dimethyl ester at the diglucuronide moiety (**3**) with ethyl chloroformate and subsequently reducing it with $NaBH_4$ as previously described.[22]

The synthesis of the amide derivatives of GL (**5**−**8**), which contain two amine residues in the carbohydrate region of the GL molecule, was carried out by transesterification of the GL dimethyl ester (**4**) with the corresponding aqueous amine at 80 °C in a sealed tube as outlined in Scheme 2.

To synthesize amines **10**−**25**, compound **4** was treated with pyridinium chlorochromate (PCC) in CH_2Cl_2 as shown in Scheme 3 to yield the key aldehyde **9**. Compounds **10**−**16** were obtained from **9** by addition of the corresponding amine and treatment with $NaBH_3CN$ in anhydrous MeOH with the pH adjusted to ∼6. Furthermore, deprotection of the sugar moiety provided the desired derivatives. Following the same procedure, compounds **17**−**24** were prepared from **9** using the corresponding alkyl (methyl, ethyl) ester of the amino acid hydrochloride salt.

In Vitro LPS-Induced HMGB1 Release Studies. The GL derivatives were tested for the inhibition of HMGB1 stimulated by LPS. Several studies have demonstrated independently that HMGB1 can be actively released from a variety of cells, including macrophage-like RAW 264.7 cells.[13] Once released, HMGB1 can bind to cell-surface receptors [e.g., the receptor for advanced RAGE, Toll-like receptor (TLR) 2, and TLR4] and mediates various cellular responses, including chemotactic cell movement and the release of proinflammatory cytokines (e.g., TNF and IL-1).[6] In other words, HMGB1 can induce TNF-α release from RAW 264.7 cell cultures activated by LPS. All of the GL derivatives and antibodies were screened and assayed for the inhibition of TNF-α production by ELISA according to the manufacturer's instructions. All compounds were tested at least twice in triplicate.

From a preliminary analysis of the results, which are summarized in Table 1, general inhibition was observed for GL derivatives **10**, **12**, **18**−**20**, **23**, and **24**, ranging from 337 to 141 μM, as compared to the leading compound **1**, which has ED_{50} = 70 μM. However, GL amides **5**−**8** showed either low solubility levels in PBS or high cell cytotoxicity. Briefly, the introduction of amine residues in the carbohydrate region of the GL molecule resulted in a loss of activity, indicating that the free carboxyl at the carbohydrate is necessary. In contrast, significantly different inhibitory activities were found for compounds **10**−**24**. Interestingly, the activity of the targeted compounds **10**−**16**, which contain the alkylamino substituents, differed and only amines **10** and **12** showed reduced inhibition. The incorporation of amino acid residues at C-30 resulted in compounds with reduced anti-HMGB1 properties (**18**−**20**, **23**, and **24**). No inhibition against HMGB1 was found for compounds **17**, **21**, and **22**. Of the seven bioactive GL derivatives, **23** exhibited the highest level of inhibition and **18** showed the lowest level. We speculated that substituents at C-30 with a certain length and electrical property might be necessary for bioactivity. It was suggested that a small change at the C-30 side chain highly impacts the HMGB1 inhibitory activity.

Table 1. Inhibitory Activities of Selective HMGB1 Antagonists against LPS-Induced TNF-α Release in RAW 264.7 Cells

compound	ED_{50} (μM)	95% confidence interval (μM)
glycyrrhizin	70	70−90
HMGB1 antibody	2.29[a]	1.7−3.4[a]
10	226	110−370
12	193	150−220
18	337	200−660
19	161	120−210
20	144	80−330
23	141	120−180
24	144	100−200

[a] μg/mL.

Pharmacological Activities in Mice. The in vivo profiles of selected compounds **17**−**20**, **23**, and **24** were evaluated using DOX-induced acute heart failure DCM mice after the ligands had been administered intraperitoneally (ip) (Figure 1). Therapeutic blockade of HMGB1 induced protective effects on cardiac dysfunctions, and the animal survival rate by the GL derivatives was measured. GL derivative **17** did not possess anti-HF activity, which was supported by its lack of efficacy in the HMGB1 release assay, as shown previously (Table 1). Compound **18** (ED_{50} = 161 μM) displayed an ip potency similar to that of the parent compound **1**. It did not increase the survival rate or ejection fraction significantly, but it elicited an improvement in the maximum ascending and descending rate of the left ventricle (LV) pressure. As observed in Figure 1A and Figure 1B, the protective effects on cardiac dysfunctions and the animal survival rate of GL derivatives **19**, **20**, and **23** were not significantly higher than that of **1**. Treatment of DCM mice with **24** significantly increased the animal survival rate (Figure 1A) compared with the DOX plus phosphate-buffered saline (PBS) treated group and improved cardiac dysfunction as measured by different parameters (Figure 1B).

GL derivatives **23** and **24** were evaluated using the DOX-induced chronic heart failure DCM mouse model. Treatment with **23** increased the animal survival rate and markedly ameliorated DOX-induced LV dysfunction, including affecting the diastolic interventricular septum, systolic interventricular

dx.doi.org/10.1021/jm301248y | J. Med. Chem. 2013, 56, 97−108

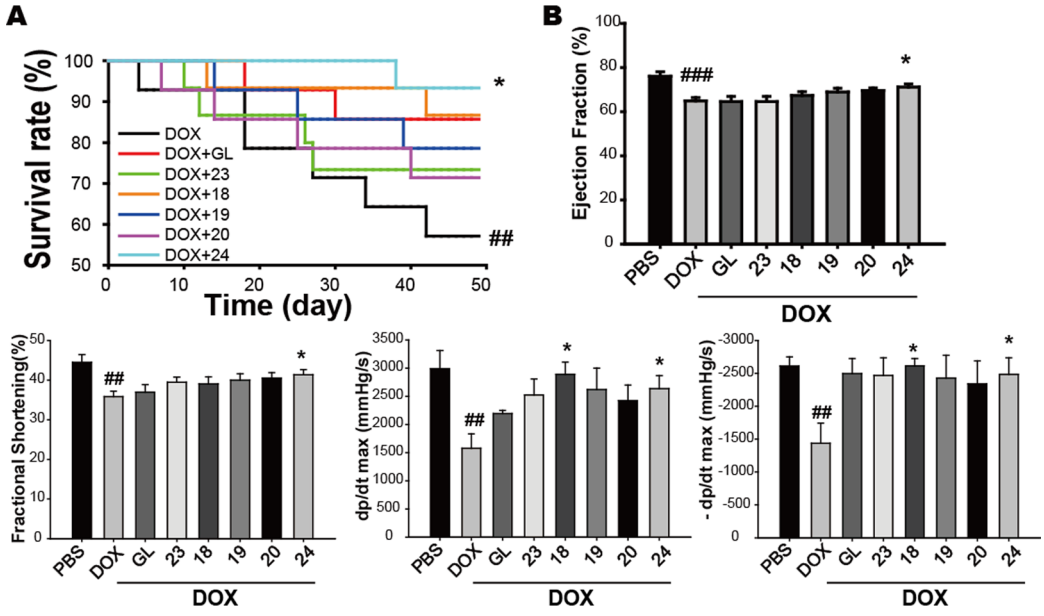

Figure 1. Therapeutic blockade of HMGB1 by GL or its derivatives induces protective effects on cardiac dysfunctions and animal survival in acute DCM mice. Ten days after DCM (injection of one high dose of DOX) was induced, the animals were treated with the indicated agent once per day. Fifty days later, the mice were studied and sacrificed. (A) Survival rate curves were generated using the Kaplan–Meier method and compared using a log rank test (n = 15/group). (B) Effects of GL derivatives on DOX-induced cardiac dysfunctions. EF = ejection fraction; FS = fractional shortening; $+dp/dt_{max}$ = maximum ascending rate of LV pressure; $-dp/dt_{max}$ = maximum descending rate of LV pressure. Data are the mean ± SEM: (##) P < 0.01 versus PBS-treated group; (*) P < 0.05, (**) P < 0.01 versus DOX plus PBS-treated group.

septum, ejection fraction, fractional shortening, and LV diastolic anterior wall (Figure 2). Conversely, **24** did not show any cardioprotective effect.

Compounds **23** and **24** were found to be potent antagonists of CHF and AHF, respectively, as indicated by the increased survival rate and amelioration of the cardioprotective effect. However, both of these compounds showed comparable inhibition of HMGB1 in vitro. Indeed, the observation of neither high nor low HMGB1 inhibitory activity in vitro with cell-based results was associated with anti-HF activity. Thus, molecular modeling studies were performed to explain the subtle difference in the interactions between the GL derivatives and HMG boxes.

Modeling Studies. To get deep insight into the mechanism for the HMGB1 inhibitory activities of GL, **23**, and **24** and the anti-HF effects of **23** and **24**, molecular modeling studies were performed to explore the detailed interactions of these compounds with the A box and B box, respectively. The crystal structures of the A box [Protein Data Bank (PDB) entry 1aab][23] and B box (PDB entry 1hmf)[24] were downloaded from the Protein Data Bank (http://www.rcsb.org/pdb/). Molecular dockings were performed with Gold 5.1.[25] Molecular dynamics (MD) simulations were then performed on the docking complexes using the GROMACS package[26] to refine the models.

Molecular Docking with the A Box. The molecular modeling results revealed that in addition to hydrophobic interactions between the cycloalkane skeleton of GL with Met12, Tyr15, Ala16, Val19, Gln20, Lys27, and Phe37, the carbonyl group at C-11 and the carboxyl group at C-30 of GL formed two hydrogen bonds with the guanidinium group of Arg23 and the hydroxyl group of Ser41, respectively. Moreover, the complex was further stabilized by an electrostatic interaction between the C-30 carboxyl group of GL and the hydroxyl group of Tyr15 (Figure 3A). This result is generally consistent with that from the study of Mollica and co-workers, which found higher chemical-shift differences for these residues in an NMR assay.[19] Derivatives **23** and **24** displayed binding patterns similar to that of GL because the triterpene scaffold of **23** made hydrophobic interactions with Met12, Tyr15, Ala16, Val19, Gln20, Arg23, Lys27, and Phe37, and a specific hydrogen bond was formed between the C-30 carboxyl group of **23** and the hydroxyl group of Ser41. However, the electrostatic interaction and hydrogen bonding contact between the carbonyl group at C-11 and the guanidinium group of Arg23 were not observed, which may be one of the reasons for the weaker bonding force of **23** with the A box compared with GL (Figure 3B). For **24**, hydrogen bonding with the hydroxyl group of Ser41 and hydrophobic interactions with Gly10, Met12, Ser13, Tyr15, Ala16, Gln20, Arg23, Phe37, and Ser38 were detected. In addition, no electrostatic interactions were predicted in the model (Figure 3C), which was similar to **23**. Therefore, GL performed best in the interaction with the A box.

Molecular Docking with the B Box. Phe101, Phe102, Lys113, Ile121, Ala125, and Lys126 in the active site of the B box formed hydrophobic interactions with the triterpene scaffold of GL. Moreover, the carbonyl group at C-11 of GL formed a hydrogen bond with the guanidinium group of Arg109 (Figure 4A). Compounds **23** and **24** displayed similar bonding modes, including hydrogen bonds with Arg109 and hydrophobic contacts with Phe101, Phe102, Ile121, Val 124, Ala125, and Lys126, except for additional hydrogen bonds between their sugar moieties and the amino group of Lys113 (Figure 4B and Figure 4C), which further stabilized these complexes. Therefore, **23** and **24** exhibited much stronger bonding forces with the B box than GL, which is the domain of HMGB1 that is important in cardiovascular disease treatment.

From the molecular modeling study, we can speculate that GL possesses a stronger bonding force to the A box and a

dx.doi.org/10.1021/jm301248y | J. Med. Chem. 2013, 56, 97–108

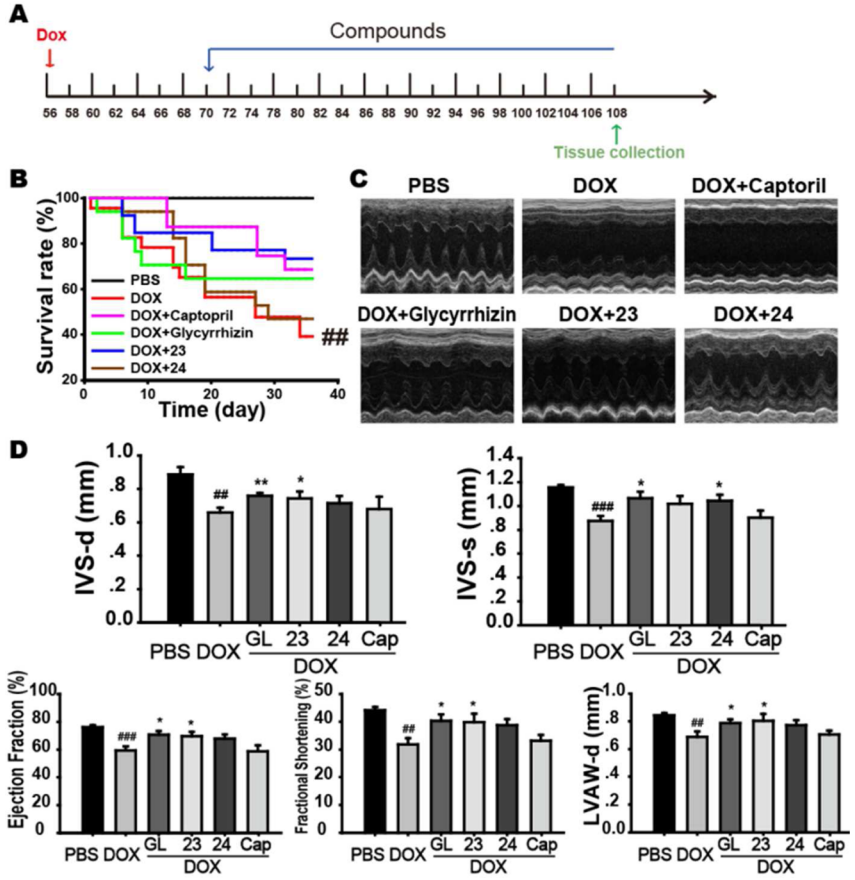

Figure 2. Inhibition of HMGB1 improves cardiac function and animal survival in DOX-induced chronic DCM. (A) Therapeutic protocol for animals with chronic DCM. Mice were treated with low doses of DOX (3.5 mg/kg) weekly for 8 weeks. Two weeks after the last DOX treatment, the animals were treated with the indicated agent once per day. (B) Survival rate curves were generated using the Kaplan–Meier method and compared using a log rank test (n = 20/group). (C) Representative images of LV M-mode echocardiograms. (D) Inhibition of HMGB1 markedly ameliorated DOX-induced LV dysfunction. IVS-d = diastolic interventricular septum; IVS-s = systolic interventricular septum; EF = ejection fraction; FS = fractional shortening; LVAW-d = left ventricular diastolic anterior wall. Data are the mean ± SEM (n = 8/group): (##) $P < 0.01$, (###) $P < 0.001$ versus PBS-treated group; (∗) $P < 0.05$ versus DOX plus PBS-treated group.

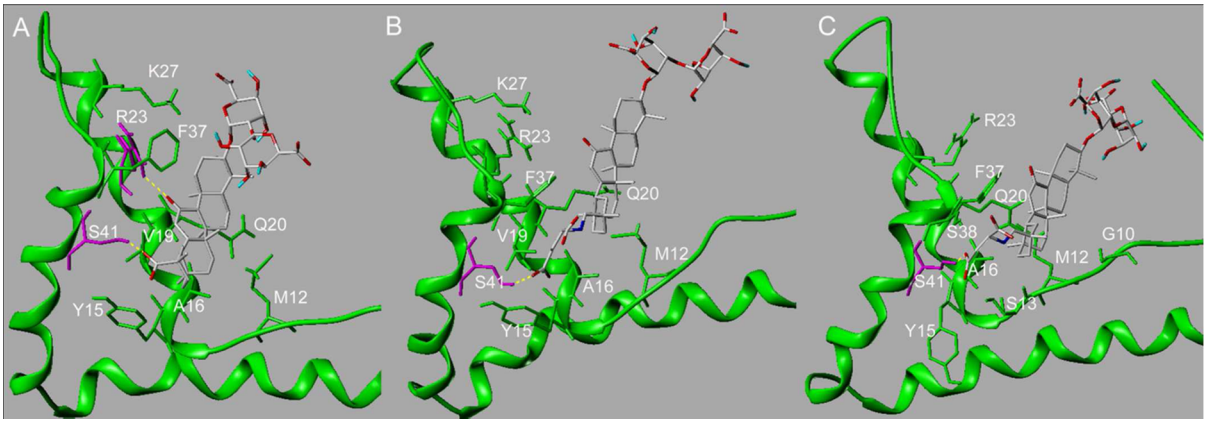

Figure 3. Predicted binding modes of GL, **23**, and **24** in the active site of the A box. (A) GL (CPK) establishes favorable van der Waals interactions with the hydrophobic side chains of Met12, Tyr15, Ala16, Val19, Gln20, Lys27, and Phe37 (green). The carbonyl group and carboxyl group of GL form two stable hydrogen bonds with the guanidinium group of Arg23 and the hydroxyl group of Ser41, respectively (magenta). The complex is further stabilized by an electrostatic interaction between the carboxyl group of GL and the hydroxyl group of Tyr15. The secondary structure of the A box is represented in green. (B) The model predicts hydrophobic interactions of the triterpene scaffold of **23** (CPK) with the side chains of Met12, Tyr15, Ala16, Val19, Gln20, Arg23, Lys27, and Phe37 (green). The carboxyl group of **23** forms a hydrogen bond with the hydroxyl group of Ser41 (magenta). (C) Similar to **23**, hydrogen bonding contacts with the hydroxyl group of Ser41 and hydrophobic interactions with Gly10, Met12, Ser13, Tyr15, Ala16, Gln20, Arg23, Phe37, and Ser38 were detected for **24** (CPK).

dx.doi.org/10.1021/jm301248y | J. Med. Chem. 2013, 56, 97–108

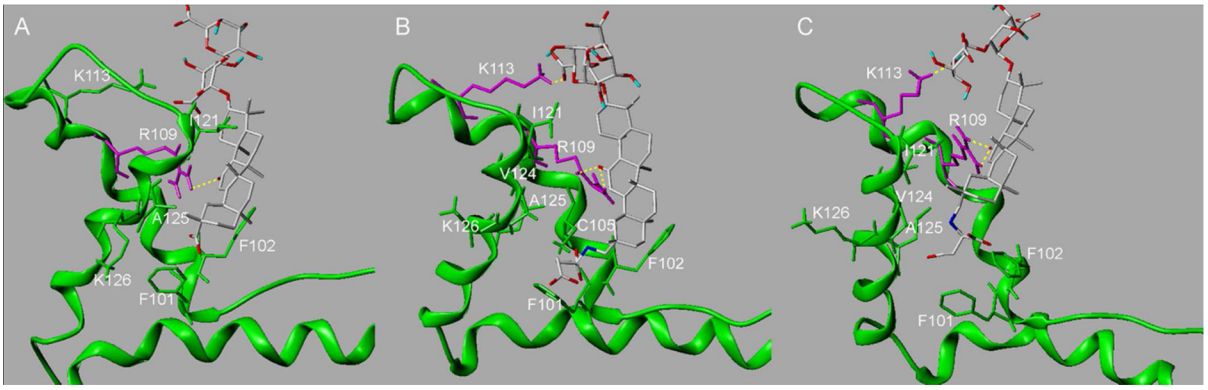

Figure 4. Predicted binding modes of GL, **23**, and **24** in the active site of the B box. (A) GL (CPK) establishes favorable van der Waals interactions with the hydrophobic side chains of Phe101, Phe102, Lys113, Ile121, Ala125, and Lys126 (green). The carbonyl group of GL at C-11 forms hydrogen bonds with the guanidinium group of Arg109 (magenta). The secondary structure of the B box is represented in green. (B, C) The two models predict the hydrophobic interactions of the cycloalkane skeletons of **23** and **24** (CPK) with the side chains of Phe101, Phe102, Ile121, Val124, Ala125, and Lys126 (green). In addition to the hydrogen bond formed between the carbonyl group of GL and the guanidinium group of Arg109 in the receptor, the sugar moieties of **23** and **24** are predicted to create stable hydrogen bonds with the amino group of Lys113 (magenta).

relatively weaker bonding force to the B box compared with compounds **23** and **24**. It has been shown that the appropriate inhibition of HMGB1 by targeted binding to the B box is efficient for cardiovascular diseases treatment.[13,16,17] Thus, **23** and **24** should show a stronger cardioprotective effect than GL, which is in accordance with the in vivo activity results. Because the A box exerts an antagonistic effect on the B box, excess interaction with the A box will weaken the inhibition of the B box.[13−15] GL, which possesses a stronger bonding force to the A box than **23** and **24**, exhibits a higher inhibitory activity on HMGB1 in vitro and a relatively weaker in vivo effect. In conclusion, a moderate bonding force with the HMG box A and relatively higher binding to the B box should result in the moderate inhibition of HMGB1 and thus a higher animal survival rate and stronger cardioprotective effect, reflecting the dual role of HMGB1 in promoting cardiac stem cell growth and differentiation and inducing myocardial cell apoptosis.

■ CONCLUSIONS

We have synthesized a series of novel GL derivatives with a C−N bond through the amino group of amines or amino acids and C-30. Compounds **23** and **24** emerged as promising HMGB1 inhibitors, facilitating the recovery of the cardiovascular functions, supported by their strong bonding forces with the B box. The finding that a small change in the GL structure produces a profound change in effectiveness of the HF treatment exemplifies the complexity of the structure−activity relationships in this series. In light of the potential applications of the effective inhibitors, it appears worthwhile to further investigate this new class of compounds with anti-HF activities.

■ EXPERIMENTAL SECTION

Chemistry. All the starting materials were of reagent grade. The solvents used for the isolation/purification of the compounds were obtained from Fisher Scientific (Pittsburgh, PA, U.S.). All reactions were carried out in oven-dried glassware under an argon atmosphere unless otherwise noted. All yields reported refer to the yields of the isolated compounds. ^{1}H NMR and ^{13}C NMR spectra were recorded using a Varian Inova-500 spectrometer (500 MHz). High-resolution mass spectra were obtained with an AccuTOF CS (JMS-T100CS, JEOL) mass spectrometer. ESI-MS was performed with an Agilent 1100 series LC-MSD-Trap-SL mass spectrometer. Silica gel TLC plates (Qing Dao Marine Chemical Factory, Qingdao, China) were used to monitor the progression of the reactions. Flash column chromatography was performed using silica gel (200−400 mesh size, Qing Dao Marine Chemical Factory, Qingdao, China). The purity of the test compounds was determined by HPLC analysis using an Agilent 1100 series instrument equipped with a DAD detector and a YMC-Pack ODS column (100 mm × 4.6 mm, 5 μm). The intensity of the major peak in the analytical HPLC trace of each target compound was ≥95% that of the combined intensities of all of the peaks detected at 254 nm. Preparative HPLC was performed on a Shimadzu instrument equipped with a LC-6AD pump and a SPD-10A detector using a YMC-PACK ODS-A column (250 mm × 20 mm, 5 μm).

Compound 3. The pentaacetate of the GL dimethyl ester at its diglucuronide moiety was prepared according to the method of Sasaki et al.[27] White powder (72% yield); ^{1}H NMR (500 MHz, pyridine) δ 5.91(1H, s, H-12), 5.34 (1H, d, J = 8 Hz, H-1″), 4.94 (1H, d, J = 7.5 Hz, H-1′), 3.79 (3H, s, OCH_3), 3.67 (3H, s, OCH_3), 3.23 (1H, br d, J = 9 Hz, H-3), 3.03 (1H, br d, J = 12.5 Hz, H-1a), 2.46 (1H, br d, J = 12 Hz, H-18), 2.15, 2.08, 2.01, 1.99, 1.98 (each 3H, s, Ac) 1.36, 1.30, 1.21, 1.18, 1.05, 1.05, 0.75 (each 3H, s, CH_3).

Compound 4. This compound was prepared as previously reported:[22] A solution of ethyl chloroformate (1 mL) in THF (5 mL) was added to a solution of the dimethyl ester pentaacetate of GL (5.4 g) and Et_3N (1.4 mL) in THF (25 mL) over the course of 30 min at −5 °C, and the mixture was stirred for 30 min at the same temperature. The precipitate was filtered and washed with THF, and the combined filtrates were added over 30 min to a solution of $NaBH_4$ (0.47 g) in H_2O (5 mL) at 10−15 °C. Then the reaction mixture was stirred at room temperature for 4 h and acidified with diluted HCl; the two layers of the reaction mixture were subsequently separated. The organic layer was washed with 10% aqueous NaOH and then dried over anhydrous Na_2SO_4. The solvent was evaporated to yield a residue, which was chromatographed on silica gel (solvent, $CHCl_3$/MeOH = 100/1) to obtain the product. White powder (58% yield); ^{1}H NMR (500 MHz, pyridine) δ 5.78 (1H, s, H-12), 5.38 (1H, d, J = 8 Hz, H-1″), 4.99 (1H, d, J = 7.5 Hz, H-1′), 3.82 (3H, s, OCH_3), 3.78 (1H, dd, J = 11, 4.5 Hz, H-30a), 3.71 (1H, dd, J = 10.5, 5.5 Hz, H-30b), 3.69 (3H, s, OCH_3), 3.26 (1H, dd, J = 11, 4.5 Hz, H-3), 3.11 (1H, br d, J = 13.5 Hz, H-1a), 2.42 (1H, s, H-9), 2.18, 2.06, 2.03, 2.01, 2.00 (each 3H, s, Ac), 1.38, 1.26, 1.23, 1.15, 1.12, 1.09, 0.82 (each 3H, s, CH_3); ^{13}C NMR (125 MHz, pyridine) δ 199.5, 170.3, 170.3, 170.1, 169.9, 169.9, 169.7, 168.3, 167.6, 128.5, 103.4, 101.2, 90.2, 77.9, 74.5, 73.1, 73.0, 72.6, 72.0, 70.6, 70.3, 65.4 (C-30), 62.0, 55.4, 52.7, 52.6, 47.3, 45.5, 43.6, 40.8, 39.8, 39.4, 37.2, 36.4, 36.0, 32.9, 32.5, 30.0, 28.7, 28.2, 27.8, 26.9, 26.7, 26.4, 23.5, 20.7, 20.5, 20.5, 20.4, 20.4, 18.8, 17.6, 16.7, 16.5. ESI-MS: m/z = 1067 $[M + Na]^+$.

General Procedures for Converting the Ester to an Amide for Compounds 5−8. The GL ester (0.1 mmol) was dissolved in

dx.doi.org/10.1021/jm301248y | J. Med. Chem. 2013, 56, 97−108

amine (2 mL), and the solution was allowed to stand at 80 °C for 4 h in a sealed tube. The solvent was then evaporated, and the resulting product was purified by preparative HPLC (CH_3CN/H_2O = 60:40, flow rate = 5 mL/min).

Compound 5. White powder (47% yield); ^{1}H NMR (500 MHz, pyridine) δ 8.25 (1H, t, J = 6 Hz, H−N), 8.12 (1H, t, J = 6 Hz, H−N), 5.77 (1H, s, H-12), 5.43 (1H, d, J = 8 Hz, H-1″), 4.84 (1H, d, J = 7.5 Hz, H-1′), 3.78 (1H, d, J = 10.5 Hz, H-30a), 3.72 (1H, d, J = 10.5 Hz, H-30b), 3.49−3.29 (4H, m, N−CH_2 × 2), 3.23 (1H, dd, J = 12, 4.5 Hz, H-3), 3.12 (1H, br d, J = 13.5 Hz, H-1a) 2.45 (1H, s, H-9), 2.26 (1H, dd, J = 13.5, 3.5 Hz), 1.42, 1.29, 1.23, 1.16, 1.10, 1.10, 0.82 (each 3H, s, CH_3); ^{13}C NMR (125 MHz, pyridine) δ 199.5, 170.7, 170.2, 170.0, 128.5, 105.6, 104.7, 88.7, 82.2, 77.6, 77.4, 76.5, 76.3, 76.2, 73.8, 73.4, 65.4, 62.1, 55.3, 47.3, 45.6, 43.7, 41.2 ($\underline{C}H_2$−N), 41.0 ($\underline{C}H_2$−N), 40.8, 39.9, 39.4, 37.3, 36.4, 36.0, 32.9, 32.5, 30.0, 28.7, 28.3, 28.0, 26.9, 26.8, 26.7, 23.5, 23.4 ($\underline{C}H_2$−CH_3), 23.2 ($\underline{C}H_2$−CH_3), 18.8, 17.6, 16.7, 16.7, 11.7 (CH_3), 11.4 (CH_3). ESI-MS: m/z = 913 $[M + Na]^+$, 925.5 $[M + Cl]^-$. HRESIMS: m/z = 889.5428 $[M - H]^-$ (calcd for $C_{48}H_{78}N_2O_{13}$, 889.5431).

Compound 6. White powder (65% yield); ^{1}H NMR (500 MHz, pyridine) δ 9.08 (1H, t, J = 6 Hz, H−N), 8.83 (1H, t, J = 6 Hz, H−N), 7.53 (2H, d, J = 6 Hz, Ar−H), 7.46 (2H, d, J = 6 Hz, Ar−H), 7.34−7.24 (4H, m, Ar−H), 7.17 (2H, m, Ar−H), 5.78 (1H, s, H-12), 5.41 (1H, d, J = 7.5 Hz, H-1″), 4.85 (1H, d, J = 7.5 Hz, H-1′), 3.78 (1H, d, J = 10.5 Hz, H-30a), 3.71 (1H, d, J = 10.5 Hz, H-30b), 3.14 (1H, dd, J = 12, 4.5 Hz, H-3), 3.09 (1H, br d, J = 13.5 Hz, H-1a), 2.43 (1H, s, H-9), 2.26 (1H, dd, J = 13.5, 3.5 Hz), 1.42, 1.22, 1.17, 1.15, 1.10, 1.00, 0.83 (each 3H, s, CH_3); ^{13}C NMR (125 MHz, pyridine) δ 199.5, 170.7, 170.1, 170.0, 139.8 (Ar−C), 139.6 (Ar−C), 128.9 (Ar−C), 128.9 (Ar−C), 128.9 (Ar−C), 128.9 (Ar−C), 128.5, 128.1 (Ar−C), 128.1 (Ar−C), 127.6 (Ar−C), 127.6(Ar−C), 127.4 (Ar−C), 127.3 (Ar−C), 105.9, 104.8, 88.7, 82.7, 77.7, 77.4, 77.1, 76.9, 76.3, 73.7, 73.2, 65.4, 62.0, 55.3, 47.3, 45.5, 43.6, 43.2 (−$\underline{C}H_2$−Ar), 42.9 (−$\underline{C}H_2$−Ar), 40.8, 39.8, 39.5, 37.2, 36.4, 36.0, 32.9, 32.5, 30.0, 28.7, 28.2, 27.9, 26.9, 26.8, 26.8, 23.6, 18.9, 17.6, 16.8, 16.7. ESI-MS: m/z = 1009 $[M + Na]^+$, 985 $[M - H]^-$. HRESIMS: m/z = 985.5417 $[M - H]^-$ (calcd for $C_{56}H_{77}N_2O_{13}$, 985.5431).

Compound 7. White powder (49% yield); ^{1}H NMR (500 MHz, pyridine) δ 8.41 (1H, t, J = 5.5 Hz, H−N), 8.37 (1H, t, J = 5.5 Hz, H−N), 5.76 (1H, s, H-12), 5.40 (1H, d, J = 8 Hz, H-1″), 4.85 (1H, d, J = 7.5 Hz, H-1′), 3.95−3.69 (10H, m), 3.23 (1H, dd, J = 11.5, 4.5 Hz, H-3), 3.08 (1H, br d, J = 13.5 Hz), 2.40 (1H, s, H-9), 2.26 (1H, dd, J = 13.5, 4 Hz), 1.39, 1.27, 1.24, 1.16, 1.13, 1.07, 0.82 (each 3H, s, CH_3); ^{13}C NMR (125 MHz, pyridine) δ 199.42, 171.0, 170.7, 169.9, 128.5, 105.8, 104.6, 88.8, 82.6, 77.5, 77.3, 76.4, 76.2, 75.7, 73.8, 73.4, 65.4, 62.0, 61.1 (O−CH_2), 60.8 (O−CH_2), 55.3, 47.3, 45.5, 43.6, 42.7 (N−CH_2), 42.3 (N−CH_2), 40.8, 39.9, 39.5, 37.2, 36.4, 36.0, 32.9, 32.5, 30.0, 28.7, 28.2, 27.9, 26.9, 26.8, 26.7, 23.5, 18.8, 17.6, 16.7, 16.6. ESI-MS: m/z = 893.5 $[M - H]^-$. HRESIMS: m/z = 893.5004 $[M - H]^-$ (calcd for $C_{46}H_{73}N_2O_{15}$, 893.5016).

Compound 8. White powder (47% yield); ^{1}H NMR (500 MHz, pyridine) δ 8.22 (1H, t, J = 6 Hz, H−N), 8.09 (1H, t, J = 6 Hz, H−N), 5.77 (1H, s, H-12), 5.43 (1H, d, J = 7.5 Hz, H-1″), 4.85 (1H, d, J = 8 Hz, H-1′), 3.77 (1H, d, J = 10.5 Hz, H-30a), 3.71 (1H, d, J = 10.5 Hz, H-30b), 3.51−3.34 (4H, m, N−CH_2 × 2), 3.23 (1H, dd, J = 12, 4.5 Hz, H-3), 3.13 (1H, br d, J = 13.5 Hz, H-1a), 2.46 (1H, s, H-9), 2.25 (1H, dd, J = 13, 3.5 Hz), 1.42, 1.30, 1.24, 1.15, 1.11, 1.10 (each 3H, s, CH_3), 0.85 (3H, t, J = 7.5 Hz, CH_3), 0.82 (3H, s, CH_3) 0.78 (3H, t, J = 7.5 Hz, CH_3); ^{13}C NMR (125 MHz, pyridine) δ 199.4, 170.6, 170.1, 170.0, 128.5, 105.7, 104.7, 88.7, 82.2, 77.6, 77.4, 76.5, 76.3, 76.2, 73.8, 73.4, 65.4 (30), 62.1, 55.3, 47.3, 45.6, 43.6, 40.8, 39.9, 39.5, 39.2 (N−CH_2), 39.0 (N−CH_2), 37.3 (22), 36.4 (20), 36.0, 32.9, 32.5, 32.3 (N−CH_2−$\underline{C}H_2$−), 31.9 (N−CH_2−$\underline{C}H_2$−), 30.0 (21), 28.7, 28.2, 28.0, 26.9, 26.9, 26.7, 23.6, 20.5 (CH_3−$\underline{C}H_2$−), 20.2 (CH_3−$\underline{C}H_2$−), 18.8, 17.6, 16.8, 16.8, 14.0 (CH_3), 13.9 (CH_3). ESI-MS: m/z = 917.6 $[M - H]^-$. HRESIMS: m/z = 917.5740 $[M - H]^-$ (calcd for $C_{50}H_{81}N_2O_{13}$, 917.5744).

Compound 9. To a solution of **4** (1.5 g) in CH_2Cl_2 (8 mL) was added PCC (659 mg) at 0 °C. After being stirred for 1 h at 0 °C, the reaction mixture was warmed to room temperature and stirred for 1 h. The reaction mixture was filtered over a celite pad and evaporated under reduced pressure to dryness. The residue was purified by flash column chromatography (petroleum/EtOAc = 1/1, v/v), which afforded **9** (1.1 g, 73% yield) as a white powder. ^{1}H NMR (500 MHz, pyridine) δ 9.50 (1H, s, CHO), 5.82 (1H, s, H-12), 5.38 (1H, d, J = 8 Hz, H-1″), 4.99 (1H, d, J = 8 Hz, H-1′), 3.82 (3H, s, OCH_3), 3.69 (3H, s, OCH_3), 3.26 (1H, dd, J = 11.5, 4.5 Hz, H-3), 3.10 (1H, br d, J = 13 Hz, H-1a), 2.42 (1H, s, H-9), 2.18, 2.07, 2.03, 2.01, 2.00 (each 3H, s, Ac), 1.41, 1.26, 1.23, 1.12, 1.06, 0.88, 0.72 (each 3H, s, CH_3); ^{13}C NMR (125 MHz, pyridine) δ 206.0 (CHO), 199.4, 170.3, 170.3, 169.9, 169.7, 168.7, 168.3, 167.6, 128.8, 103.4, 101.2, 90.3, 77.9, 74.6, 73.1, 73.0, 72.6, 72.0, 70.6, 70.3, 62.1, 55.4, 52.7, 52.6, 48.0, 47.0, 45.6, 43.4, 39.8, 39.4, 38.5, 37.4, 37.2, 32.8, 32.1, 28.6, 28.4, 27.8, 26.7, 26.4, 26.3, 23.9, 23.6, 20.7, 20.5, 20.5, 20.4, 20.4, 18.8, 17.7, 16.7, 16.5.

General Procedures for Reductive Amination Using Sodium Cyanoborohydride for Compounds 10−16. The aldehyde precursor (**9**, 250 mg) was dissolved in methanol (10 mL), and an amount of 2 equiv of amine was added. The pH of the solution was adjusted to ∼6 by adding glacial acetic acid. Then an amount of 1.2 equiv of $NaBH_3CN$ in methanol was added. The mixture was stirred at room temperature for 3 h and quenched with H_2O (10 mL). The solution was extracted with EtOAc, and the combined organic layers were washed with water, dried over anhydrous Na_2SO_4, and concentrated. Purification by preparative HPLC ($MeCN/H_2O$ = 9:1) gave the corresponding intermediate. A solution of the intermediate in 5% potassium hydroxide in $EtOH/H_2O$ (1:1, 10 mL) was stirred at room temperature for 1 h. The reaction mixture was then neutralized with ion-exchange resin (Amberlite IR-120 H^+), and the filtrate was concentrated in vacuo to yield a residue that was subjected to Sephadex LH-20 ($MeOH/H_2O$ = 1:1) to afford the product.

Compound 10. White powder (48% yield); ^{1}H NMR (500 MHz, DMSO) δ 5.57 (1H, s, H-12), 4.39 (1H, d, J = 7.5 Hz, H-1″), 4.28 (1H, d, J = 7.5 Hz, H-1′), 2.27 (1H, s, H-9), 2.10−2.05 (2H, m), 1.30, 1.02, 1.02, 0.94, 0.94 (each 3H, s, CH_3), 0.87 (3H, t, J = 7 Hz), 0.81, 0.73 (each 3H, s, CH_3); ^{13}C NMR (125 MHz, DMSO) δ 199.0, 172.4, 171.6, 169.3, 127.7, 103.9, 103.4, 87.9, 81.7, 76.3, 75.9, 75.3, 73.6, 72.0, 72.0, 61.2, 54.5, 51.8 (N−CH_2), 50.6 (C-30), 45.7, 44.9, 43.0, 41.2, 40.8, 38.9, 36.4, 35.3, 33.5, 32.2, 31.9, 28.1, 27.7, 27.4, 26.1, 26.1, 26.0, 25.4, 23.2, 23.2 ($\underline{C}H_2$−CH_3), 18.4, 17.0, 16.2, 16.2, 11.4 (CH_3). HRESI-MS: m/z = 850.4967 (calcd for $C_{45}H_{72}NO_{14}$, 850.4947). ESI-MS: m/z = 850 $[M + H]^+$, 848 $[M - H]^-$.

Compound 11. White powder (31% yield); ^{1}H NMR (500 MHz, DMSO) δ 5.50 (1H, s, H-12), 4.43 (1H, d, J = 7.5 Hz, H-1″), 4.28 (1H, d, J = 7.5 Hz, H-1′), 2.29 (1H, s, H-9), 1.32, 1.05 (each 3H, s, CH_3), 1.03 (6H, overlap, CH_3 × 2), 1.02, 0.96, 0.86, 0.80, 0.72 (each 3H, s, CH_3); ^{13}C NMR (125 MHz, DMSO) δ 199.1, 172.8, 171.6, 169.9, 127.4, 103.5, 103.2, 88.0, 80.4, 76.4, 76.1, 75.1, 73.7, 72.2, 72.2, 61.1, 54.4, 49.7 (N−CH), 49.4 (C-30), 46.2, 44.9, 43.0, 41.50, 40.8, 38.7, 36.4, 35.6, 33.8, 32.2, 31.9, 30.7, 28.3, 28.1, 27.5, 26.1, 26.0, 25.4, 23.14, 21.7 (CH_3), 21.7 (CH_3), 18.4, 17.0, 16.20, 16.2. HRESI-MS: m/z = 850.4960 (calcd for $C_{45}H_{72}NO_{14}$, 850.4947). ESI-MS: m/z = 850 $[M + H]^+$, 848 $[M - H]^-$.

Compound 12. White powder (45% yield); ^{1}H NMR (500 MHz, DMSO) δ 5.58 (1H, s, H-12), 4.41 (1H, d, J = 7.5 Hz, H-1″), 4.30 (1H, d, J = 7.5 Hz, H-1′), 2.27 (1H, s, H-9), 1.31, 1.02, 1.02, 0.95, 0.93, 0.82, 0.70 (each 3H, s, CH_3); ^{13}C NMR (125 MHz, DMSO) δ 199.0, 171.8, 170.7, 169.3, 127.7, 104.6, 103.5, 88.0, 82.5, 76.2, 75.9, 75.7, 75.2, 74.1, 71.8, 71.8, 61.2, 57.6 (N−CH), 54.5, 48.4, 45.6, 43.0, 40.9, 40.8, 38.8, 36.3, 35.2, 33.2, 32.1, 31.9, 30.1, 28.6, 28.0, 27.3 (CH_2), 27.3 (CH_2), 26.0, 25.9, 25.5, 25.0 (CH_2), 24.5 (CH_2), 24.5 (CH_2), 23.2, 18.4, 17.0, 16.3, 16.1. HRESI-MS: m/z = 890.5275 (calcd for $C_{48}H_{76}NO_{14}$, 890.5260). ESI-MS: m/z = 890 $[M + H]^+$, 888 $[M - H]^-$.

Compound 13. White powder (53% yield); ^{1}H NMR (500 MHz, pyridine) δ 7.63 (2H, m, Ar−H), 7.39 (2H, m, Ar−H), 7.33 (1H, m, Ar−H), 5.66 (1H, s, H-12), 5.43 (1H, d, J = 7.5 Hz, H-1″), 5.04 (1H, d, J = 7.5 Hz, H-1′), 4.63−4.26 (10H, m), 3.31 (1H, br d, J = 11.5 Hz, H-3), 3.06 (1H, br d, H-30a), 3.01 (1H, br d, J = 13 Hz, H-1a), 2.87 (1H, br d, J = 11.5 Hz, H-30), 2.35 (1H, s, H-9), 2.28 (1H, m), 1.39,

dx.doi.org/10.1021/jm301248y | J. Med. Chem. 2013, 56, 97−108

1.30, 1.23, 1.18, 1.13, 0.97, 0.69 (each 3H, s, CH_3); ^{13}C NMR (125 MHz, pyridine) δ 199.4, 172.5, 172.2, 168.6, 134.8 (Ar−C), 130.1 (Ar−C), 130.1 (Ar−C), 129.2 (Ar−C), 129.2 (Ar−C), 128.8 (Ar−C), 128.8, 106.9, 105.1, 89.1, 84.5, 78.5, 77.7, 77.6, 77.5, 76.9, 73.3, 73.1, 62.0, 55.4, 52.8 (Ar−$\underline{C}H_2$−N), 51.7 (C-30), 46.8, 45.4, 43.5, 42.1, 39.9, 39.4, 37.2, 35.9, 34.1, 32.8, 32.2, 30.6, 28.4, 28.1, 27.8, 26.7, 26.6, 26.5, 23.4, 18.7, 17.6, 16.8, 16.7. HRESI-MS: m/z = 898.4924 (calcd for $C_{49}H_{72}NO_{14}$, 898.4947). ESI-MS: m/z = 898 $[M + H]^+$, 896 $[M - H]^-$.

Compound 14. White powder (37% yield); ^1H NMR (500 MHz, pyridine) δ 5.77 (1H, s, H-12), 5.42 (1H, d, J = 7.5 Hz, H-1″), 5.03 (1H, d, J = 7.5 Hz, H-1′), 4.62−4.26 (8H, m), 3.35 (1H, br d, J = 8 Hz, H-3), 3.28 (1H, m, H-30a), 3.04 (1H, br d, J = 12.5 Hz, H-1a), 2.77 (1H, m), 2.72 (1H, m), 2.40 (1H, s, H-9), 2.20−2.00 (5H, m), 1.38, 1.35, 1.24, 1.20, 1.07, 1.04, 0.85 (each 3H, s, CH_3); ^{13}C NMR (125 MHz, pyridine) δ 199.5, 173.4, 172.2, 167.3, 128.7, 107.0, 105.1, 88.9, 84.7, 78.4, 77.8, 77.8, 77.6, 76.9, 73.4, 73.3, 62.1, 60.8 (N−CH), 55.4, 52.4 (C-30), 47.1, 45.5, 43.6, 42.1, 39.9, 39.6, 37.2, 36.3, 34.4, 32.9, 32.4, 32.4 (CH_2), 32.2 (CH_2), 31.1, 28.7, 28.5, 28.1, 26.8, 26.7, 26.6, 24.3 (CH_2), 24.3 (CH_2), 23.5, 18.7, 17.6, 16.9, 16.8. HRESI-MS: m/z = 876.5100 (calcd for $C_{47}H_{74}NO_{14}$, 876.5104). ESI-MS: m/z = 876 $[M + H]^+$, 874 $[M - H]^-$.

Compound 15. White powder (42% yield); ^1H NMR (500 MHz, pyridine) δ 5.77 (1H, s, H-12), 5.44 (1H, d, J = 7.5 Hz, H-1″), 5.05 (1H, d, J = 7.5 Hz, H-1′), 4.67−4.25 (8H, m), 3.64 (2H, br s), 3.46 (2H, m), 3.32 (1H, br d, J = 11.5), 3.16 (1H, br s), 3.01 (1H, br d, J = 13.5 Hz), 2.79 (2H, br s), 2.43 (2H, m), 2.37 (1H, s, H-9), 2.30−2.21 (2H, m), 2.09−1.97 (2H, m), 1.84−1.03 (4H, m), 1.40, 1.32, 1.24, 1.18, 1.00, 1.00, 0.83 (each 3H, s, CH_3); ^{13}C NMR (125 MHz, pyridine) δ 199.3, 172.4, 172.1, 168.3, 128.9, 107.0, 105.1, 89.1, 84.6, 78.5, 77.7, 77.6, 77.5, 76.9, 73.3, 73.1, 66.8 (CH_2−O−CH_2), 66.8 (CH_2−O−CH_2), 62.0, 55.3, 54.0 (HN−CH_2−$\underline{C}H_2$−N), 53.7 (CH_2−N−CH_2), 53.7 (CH_2−N−CH_2), 52.5 (HN−$\underline{C}H_2$−CH_2−N), 46.7, 45.5, 45.2 (C-30), 43.5, 42.4, 39.9, 39.4, 37.1, 35.9, 34.1, 32.8, 32.3, 30.1, 28.3, 28.0, 27.7, 26.7, 26.5, 26.4, 23.4, 18.7, 17.5, 16.8, 16.7. HRESIMS: m/z = 921.5227 (calcd for $C_{55}H_{73}N_2O_{10}$, 921.5260). ESI-MS: m/z = 921 $[M + H]^+$, 919 $[M - H]^-$.

Compound 16. White powder (31% yield); ^1H NMR (500 MHz, pyridine) δ 8.64 (1H, m, Ar−H), 7.12 (1H, m, Ar−H), 5.76 (1H, s, H-12), 5.42 (1H, d, J = 7.5 Hz, H-1″), 5.04 (1H, d, J = 7.5 Hz, H-1′), 4.62−4.28 (8H, m), 3.33 (3H, m), 3.17 (3H, m), 3.03 (1H, br d, J = 11.5 Hz), 2.82 (1H, m), 2.39 (1H, s, H-9), 1.37, 1.35, 1.24, 1.20, 1.08, 1.03, 0.81 (each 3H, s, CH_3); ^{13}C NMR (125 MHz, pyridine) δ 199.4, 172.3, 172.2, 169.3, 161.9 (Ar−C), 149.4 (Ar−C), 136.9 (Ar−C), 128.6, 123.9 (Ar−C), 121.9 (Ar−C), 107.0, 105.1, 89.0, 84.7, 78.4, 77.7, 77.6, 77.5, 77.0, 73.4, 73.1, 62.1, 55.4, 53.4 (N−CH_2), 47.0, 46.2 (C-30), 45.5, 43.5, 41.9, 40.0, 39.6, 37.2 ($\underline{C}H_2$−Ar), 37.2, 36.2, 34.6, 32.9, 32.4, 32.0, 28.6, 28.6, 28.1, 26.8, 26.8, 26.6, 23.6, 18.8, 17.6, 16.9, 16.8. HRESIMS: m/z = 913.5055 (calcd for $C_{49}H_{73}N_2O_{14}$, 913.5056). ESI-MS: m/z = 913 $[M + H]^+$, 911 $[M - H]^-$.

General Procedures for Reductive Amination Using Sodium Cyanoborohydride for Compounds 17−24. The aldehyde precursor (**9**, 250 mg) was dissolved in methanol (10 mL), and an amount of 2 equival of L-amino acid methyl (ethyl) ester hydrochloride was added, followed by the addition of 1.2 equiv of $NaBH_3CN$ in methanol. The mixture was stirred at room temperature for 3 h and quenched with water (10 mL). The solution was extracted with CH_2Cl_2, and the combined organic layers were washed with water, dried over anhydrous Na_2SO_4, and concentrated. Purification by preparative HPLC (MeCN/H_2O = 9:1) gave the corresponding intermediate. A solution of the intermediate in 5% potassium hydroxide in EtOH/H_2O (1:1, 10 mL) was stirred at room temperature for 1 h. The reaction mixture was then neutralized with ion-exchange resin (Amberlite IR-120 H^+), and the filtrate was concentrated in vacuo to yield a residue that was subjected to Sephadex LH-20 (MeOH/H_2O = 1:1) to afford the product.

Compound 17. White powder (59% yield); ^1H NMR (500 MHz, DMSO) δ 5.73 (1H, s, H-12), 4.45 (1H, d, J = 7.5 Hz, H-1″), 4.37 (1H, d, J = 7.5 Hz, H-1′), 2.74(1H, br d, J = 11 Hz), 2.54 (1H, br d, J = 12 Hz), 2.28 (1H, s, H-9), 1.31, 1.02, 1.02, 0.96, 0.93, 0.80, 0.70 (each 3H, s, CH_3); ^{13}C NMR (125 MHz, DMSO) δ 199.2, 170.5, 170.1, 169.2, 167.5 (CO), 127.9, 104.8, 103.6, 88.2, 82.7, 76.3, 76.0, 75.7, 75.5, 75.0, 71.6, 71.4, 61.1, 54.4, 52.4 (N−$\underline{C}H_2$−CO), 50.1 (C-30), 45.3, 44.9, 42.9, 39.9, 39.0, 38.6, 36.3, 35.2, 33.4, 32.2, 31.8, 31.0, 28.1, 27.3, 27.2, 26.0, 26.0, 25.7, 23.2, 18.4, 17.0, 16.2, 16.0. HRESI-MS: m/z = 866.4545 (calcd for $C_{44}H_{68}NO_{16}$, 866.4533). ESI-MS: m/z = 866 $[M + H]^+$, 864 $[M - H]^-$.

Compound 18. White powder (42% yield); ^1H NMR (500 MHz, DMSO) δ 5.82 (1H, s, H-12), 4.45 (1H, d, J = 7.5 Hz, H-1″), 4.33 (1H, d, J = 7.5 Hz, H-1′), 2.84 (1H, br d, J = 12.5 Hz), 2.58 (1H, m), 2.28 (1H, s, H-9), 1.32 (3H, s, CH_3), 1.31 (3H, d, J = 8 Hz, CH-$C\underline{H}_3$), 1.02, 1.02, 0.95, 0.93, 0.79, 0.70 (each 3H, s, CH_3); ^{13}C NMR (125 MHz, DMSO) δ 199.2, 170.3, 170.1, 169.2, 167.9 (CO), 127.9, 104.7, 103.6, 88.2, 82.6, 76.1, 75.7, 75.5, 75.0, 72.7, 71.5, 61.2, 58.3 (N−$\underline{C}H$−CO), 54.4, 51.2 (C-30), 45.2, 44.9, 42.9, 39.9, 39.0, 38.6, 36.3, 35.4, 33.4, 32.2, 31.8, 31.6, 28.2, 27.4, 27.2, 26.0, 26.0, 25.6, 23.2, 18.4, 17.0, 16.4 (CH_3), 16.2, 16.0. HRESI-MS: m/z = 880.4687 (calcd for $C_{45}H_{70}NO_{16}$, 880.4689). ESI-MS: m/z = 880 $[M + H]^+$, 878 $[M - H]^-$.

Compound 19. White powder (42% yield); ^1H NMR (500 MHz, DMSO) δ 5.72 (1H, s, H-12), 4.46 (1H, d, J = 7.5 Hz, H-1″), 4.37 (1H, d, J = 7.5 Hz, H-1′), 2.90 (1H, br d, J = 12 Hz), 2.64 (1H, br d, J = 12.5 Hz), 2.54 (1H, br d, J = 13 Hz), 2.29 (1H, s, H-9), 2.21 (1H, m), 2.07 (1H, m), 1.32, 1.02, 1.02, 0.95, 0.93, 0.80, 0.70 (each 3H, s, CH_3); ^{13}C NMR (125 MHz, DMSO) δ 199.2, 170.6, 170.1, 169.6, 169.3 (CO), 127.7, 104.7, 103.5, 88.2, 82.7, 76.2, 76.0, 75.7, 75.2, 75.0, 71.6, 71.4, 64.6 ($\underline{C}H_2OH$), 61.1, 60.6 (N−$\underline{C}$−CO), 54.3, 51.7 (C-30), 45.4, 44.9, 42.9, 39.9, 39.0, 38.6, 36.3, 35.4, 33.6, 32.2, 31.8, 31.3, 28.2, 27.5, 27.2, 26.0, 26.0, 25.7, 23.2, 18.4, 17.0, 16.3, 16.0. HRESI-MS: m/z = 896.4653 (calcd for $C_{45}H_{70}NO_{16}$, 896.4638). ESI-MS: m/z = 896 $[M + H]^+$, 894 $[M - H]^-$.

Compound 20. White powder (55% yield); ^1H NMR (500 MHz, DMSO) δ 10.8 (1H, s, N−H), 7.55 (1H, d, J = 8 Hz, Ar−H), 7.31(1H, d, J = 8 Hz, Ar−H), 7.15 (1H, br s, Ar−H), 7.04 (1H, t, J = 7, 8 Hz, Ar−H), 6.96 (1H, t, J = 7, 8 Hz, Ar−H), 5.55 (1H, s, H-12), 4.46 (1H, d, J = 7.5 Hz, H-1″), 4.36 (1H, d, J = 7.5 Hz, H-1′), 2.64 (1H, br d, J = 11.5 Hz), 2.54 (1H, br d, J = 13 Hz), 2.27 (1H, s, H-9), 2.02 (1H, m), 1.94 (1H, m), 1.29, 1.01, 1.00, 0.93, 0.81, 0.70, 0.70 (each 3H, s, CH_3); ^{13}C NMR (125 MHz, DMSO) δ 199.1, 173.0 (CO), 170.6, 170.1, 169.5, 136.2 (Ar−C), 127.5, 127.3 (Ar−C), 123.8 (Ar−C), 121.0 (Ar−C), 118.4 (Ar−C), 118.4 (Ar−C), 111.5 (Ar−C), 110.1 (Ar−C), 104.2, 103.5, 88.2, 82.6, 76.2, 76.0, 75.7, 75.2, 75.0, 71.6, 71.4, 63.1 (N−$\underline{C}H$−CO), 61.1, 54.4, 51.7 (C-30), 45.7, 44.9, 42.9, 39.9, 39.0, 38.5, 36.3, 35.3, 33.8, 32.2, 31.7, 30.9 (CH−$\underline{C}H_2$), 28.1, 27.6, 27.5, 27.2, 26.0, 26.0, 25.7, 23.1, 18.4, 17.0, 16.3, 16.0. HRESI-MS: m/z = 995.5143 (calcd for $C_{53}H_{75}N_2O_{16}$, 995.5151). ESI-MS: m/z = 995 $[M + H]^+$, 993 $[M - H]^-$.

Compound 21. White powder (63% yield); ^1H NMR (500 MHz, pyridine) δ 7.51 (2H, t, J = 6 Hz, Ar−H), 7.29 (2H, m, Ar−H), 7.23 (1H, overlap, Ar−H), 5.91 (1H, s, H-12), 5.44 (1H, d, J = 7.5 Hz, H-1″), 5.06 (1H, d, J = 7.5 Hz, H-1′), 4.67−4.56 (4H, m), 4.42 (1H, t), 4.35−4.25 (3H, m), 3.33 (3H, m), 3.03 (2H, m), 2.38 (1H, s, H-9), 2.29 (1H, dd, J = 10, 4 Hz), 2.23 (1H, br d, J = 14 Hz), 1.40, 1.32, 1.24, 1.18, 1.02, 0.98, 0.72 (each 3H, s, CH_3); ^{13}C NMR (125 MHz, pyridine) δ 199.5, 176.7 (CO), 172.4, 172.1, 169.5, 135.8 (Ar−C), 130.0 (Ar−C), 130.0 (Ar−C), 128.6, 128.6 (Ar−C), 128.6 (Ar−C), 126.8 (Ar−C), 107.0, 105.1, 89.2, 84.5, 78.5, 77.7, 77.6, 77.5, 76.9, 73.3, 73.1, 64.7 (N−$\underline{C}H$−CO), 62.0, 55.4, 52.9 (C-30), 46.6, 45.5, 43.4, 41.1, 40.0 (CH−$\underline{C}H_2$), 39.9, 39.5, 37.2, 36.2, 34.6, 32.9, 32.3, 31.9, 28.6, 28.6, 28.1, 26.8, 26.8, 26.7, 23.5, 18.7, 17.6, 16.8, 16.7. HRESI-MS: m/z = 956.4999 (calcd for $C_{51}H_{74}NO_{16}$, 956.5002). ESI-MS: m/z = 954 $[M - H]^-$.

Compound 22. White powder (33% yield); ^1H NMR (500 MHz, pyridine) δ 7.45 (2H, d, J = 8 Hz, Ar−H), 7.12 (2H, d, J = 8 Hz, Ar−H), 5.97 (1H, s, H-12), 5.44 (1H, d, J = 7.5 Hz, H-1″), 5.05 (1H, d, J = 7.5 Hz, H-1′), 4.67−4.56 (4H, m), 4.42 (1H, t), 4.35−4.25 (3H, m), 3.40−3.30 (3H, m), 3.04 (2H, m), 2.79 (1H, m), 2.37 (1H, s, H-9), 2.27 (2H, m), 2.09−1.95 (2H, m), 1.39, 1.31, 1.23, 1.18, 1.10, 0.97, 0.72 (each 3H, s, CH_3); ^{13}C NMR (125 MHz, pyridine) δ 199.6, 176.3 (CO), 172.4, 172.1, 169.6, 157.7 (Ar−C), 135.1 (Ar−C), 131.2 (Ar−

dx.doi.org/10.1021/jm301248y | J. Med. Chem. 2013, 56, 97−108

C), 131.2 (Ar−C), 128.7, 116.2 (Ar−C), 116.2 (Ar−C), 107.0, 105.1, 89.1, 84.6, 78.5, 77.7, 77.6, 77.5, 76.9, 73.3, 73.0, 65.0 (N−C−CO), 62.0, 55.4, 52.9 (C-30), 46.6, 45.5, 43.4, 41.3, 39.9, 39.4, 38.7 (CH−CH_2), 37.2, 36.2, 34.7, 32.8, 32.3, 31.9, 28.5, 28.4, 28.1, 26.8, 26.7, 26.6, 23.5, 18.7, 17.6, 16.9, 16.8. HRESI-MS: m/z = 972.4949 (calcd for $C_{51}H_{74}NO_{17}$, 972.4951). ESI-MS: m/z = 972 $[M + H]^+$, 970 $[M - H]^-$.

Compound 23. White powder (47% yield); ^{1}H NMR (500 MHz, pyridine) δ 5.93 (1H, s, H-12), 5.44 (1H, d, J = 7.5 Hz, H-1″), 5.06 (1H, d, J = 7.5 Hz, H-1′), 4.64−4.56 (4H, m), 4.42 (1H, t), 4.35−4.25 (3H, m), 3.73 (1H, m), 3.33 (1H, br d, J = 11.5 Hz, H-3), 3.07−2.96 (5H, m), 2.57 (1H, m), 2.40 (1H, s, H-9), 2.29 (2H, m), 2.08−1.99 (2H, m), 1.40, 1.34, 1.24, 1.19, 1.10, 0.99, 0.75 (each 3H, s, CH_3); ^{13}C NMR (125 MHz, pyridine) δ 199.6, 177.6 (CH_2−CO), 175.9 (CH−CO), 172.4, 172.1, 169.7, 128.6, 107.0, 105.1, 89.2, 84.6, 78.5, 77.8, 77.6, 77.5, 76.9, 73.3, 73.1, 62.7 (N−CH−CO), 62.0, 55.4, 53.0 (C-30), 46.7, 45.5, 43.5, 41.5, 40.0, 39.5, 37.2, 36.3, 34.8, 32.9, 32.3, 32.1 (CH_2−CO), 31.9, 28.6, 28.6 28.1 (CH−CH_2), 28.1, 26.8, 26.8, 26.7, 23.5, 18.7, 17.6, 16.9, 16.8. HRESI-MS: m/z = 938.4769 (calcd for $C_{47}H_{72}NO_{18}$, 938.4744). ESI-MS: m/z = 938 $[M + H]^+$, 936 $[M - H]^-$.

Compound 24. White powder (42% yield); ^{1}H NMR (500 MHz, pyridine) δ 5.99 (1H, s, H-12), 5.44 (1H, d, J = 7.5 Hz, H-1″), 5.05 (1H, d, J = 7.5 Hz, H-1′), 4.67−4.56 (4H, m), 4.42 (1H, t), 4.35−4.24 (4H, m), 3.40 (1H, dd, J = 11, 4.5 Hz), 3.32 (2H, m), 3.20 (1H, br d, J = 11 Hz), 3.03 (1H, br d, J = 13.5 Hz), 2.85 (1H, d, J = 10.5 Hz), 2.38 (1H, s, H-9), 2.35 (1H, m), 2.30 (1H, br d, J = 10 Hz), 2.03 (2H, m) 1.39, 1.32, 1.23, 1.18, 1.12, 0.98, 0.76 (each 3H, s, CH_3); ^{13}C NMR (125 MHz, pyridine) δ 199.6, 175.6 (CH_2−CO), 174.0 (CH−CO), 172.4, 172.1, 169.5, 128.7, 106.9, 105.1, 89.1, 84.5, 78.5, 77.7, 77.6, 77.5, 76.9, 73.3, 73.0, 62.0, 59.6 (N−C−CO), 55.4, 52.8 (C-30), 46.6, 45.5, 43.4, 41.3, 39.9, 39.4, 38.1 (CH−CH_2), 37.2, 36.2, 34.6, 32.8, 32.3, 31.9, 28.5, 28.4, 28.1, 26.7, 26.7, 23.4, 18.7, 17.6, 16.9, 16.8. HRESI-MS: m/z = 924.4581 (calcd for $C_{46}H_{70}NO_{18}$, 924.4587). ESI-MS: m/z = 924 $[M + H]^+$, 922 $[M - H]^-$.

Biological Assays/Pharmacology. Reference compounds, medium, and other cell culture reagents were purchased from Sigma-Aldrich (Milan, Italy).

In Vitro HMGB1 Inhibitory Activities. Cell Culture and Stimulation. Murine macrophage-like RAW 264.7 cells (American Type Culture Collection, U.S.) were cultured in RPMI 1640 medium supplemented with 10% heat inactivated fetal bovine serum (Gemini, Calabasas, U.S.) and 2 mM glutamine in a humidified incubator with 5% CO_2 and 95% room air. To evaluate the effect of HMGB1, the RAW 264.7 cells were stimulated with LPS (0.01 ng/mL) for 16 h.[28,29] The TNF-α released into the cell culture supernatants was quantitated using a commercially available ELISA kit (catalog no. MTA00, R&D Systems) according to the manufacturer's instructions. A HMGB1 neutralization antibody and the compounds were added to the medium 2 h before LPS stimulation at the indicated concentrations.

Anti-Heart-Failure Activities. Animal Model and Treatments. Male C57BL/6J mice were purchased from Vital River Lab Animal Technology, Co. Ltd. (Beijing, China) and maintained under standard conditions in an animal facility at the Institute of Materia Medica. Animal care and experimentation were conducted in accordance with guidelines of the Institutional Committee for the Ethics of Animal Care and Treatment in Biomedical Research of the Chinese Academy of Medical Sciences.

Acute heart failure was induced with a single ip injection of DOX at a dose of 10 mg/kg. The mice were treated with GL, its derivatives, captopril, or vehicle once per day from day 10 after the injection of DOX. Sixty days after the DOX injection, the mice were anesthetized, and the LV structural and functional changes were observed by echocardiography and hemodynamic measurements. Chronic heart failure was induced by ip injection of DOX at a dose of 3.5 mg/kg for 8 weeks. The mice were treated with GL, its derivatives, captopril, or vehicle once per day from day 70. Thirty-five days later, the mice were anesthetized, and the LV structural and functional changes were observed by echocardiography.

Echocardiographic and Hemodynamic Measurements. At the end of experiment, the mice were anesthetized and transthoracic echocardiography was performed using a Vevo 770 high resolution imaging system (VisualSonics) with a 30 MHz image transducer. Measurements were taken as described previously.[30] After the cardiac echocardiography, a PE-10 catheter (Becton Dickinson, U.S.) was inserted into the aorta and LV through the right common carotid artery for continuous registration of arterial and LV pressure using a MPA2000 physiological signal acquiring system (Alcolt Biotech). The maximum ascending and descending rate of the LV pressure ($\pm dp/dt_{max}$) were measured as the representative index of the LV systolic and diastolic function.[31]

Modeling Studies. The target proteins were prepared by removing water molecules and adding all hydrogen atoms and Amber7 charges. Then energy minimizations were performed in SYBYL (Tripos Inc., St. Louis, MO), using steepest descent (SD) calculations with an embedded Amber7 force field for 5000 iterations.[32] In this procedure, heavy atoms were tethered to relieve possible steric clashes and overlaps of the hydrogen atoms. Conjugated gradient (CG) minimizations were then carried out until the systems converged to less than 0.05 kcal mol^{-1} Å^{-1} for the gradient. Other miscellaneous parameters were assigned to their default values in SYBYL. In the CG minimization procedure, heavy atoms and the backbone were tethered successively, and then the whole structure was set to free.

The 3D structures of GL, **23**, and **24** were built with the SYBYL-Sketch module. Hydrogen atoms and Gasteiger−Hükel atomic charges were added. Then energy minimizations were performed with the SYBYL compute/minimize module using POWELL calculations with a Tripos force field for rms less than 0.01 kcal mol^{-1}.[33] The final coordinates were stored in mol2 files.

GOLD utilizes a genetic algorithm (GA) to create putative poses for a single ligand. The program considers side chain flexibility and local backbone movement during docking. In this procedure, the molecular dockings were centered on (−0.85, −6.44, −0.87) for the A box and (−3.37, 7.47, 4.85) for the B box. The maximum number of energy evaluations was set to 25 000 000, and 50 conformational binding modes for each ligand were generated at the active site. The top-10 ranked poses identified by the native scoring functions of the tested programs were chosen for further analysis. Other parameters were set as defaults. The default radius defined the grid box. To further accelerate the calculation, GA docking was stopped when the top three solutions were within 1.5 Å rmsd of each other.

In the MD procedure, the simulations were carried out using periodic boundary conditions and the models were immersed in a cubic box (0.80 × 0.80 × 0.80 nm^3) of extended SPC216 water molecules. The solvated system was neutralized by adding chloride ions whose positions were randomly chosen in the simulation. Standard GROMACS amino acid residue topology and parameters based on the Gromacs force field were used. The topology and parameter files for GL, **23**, and **24** were obtained using the Dundee ProDrg Server (http://davapc1.bioch.dundee.ac.uk/prodrg/index.html). After energy minimization with the steepest decent method, the system was subjected to equilibration at 300 K and normal pressure for 100 ps under the conditions of position restraints for heavy atoms. Next, 100 ps MD simulations with restrained protein main chains and Cα atoms were performed step by step. Finally, the systems were subjected to free simulations under the same conditions for 1000 ps. Then the average structures were further refined by steepest decent and conjugate gradient energy minimizations sequentially.

■ ASSOCIATED CONTENT

Ⓢ Supporting Information

NMR (^{1}H and ^{13}C) spectra of compounds, spectroscopic data for intermediates, inhibitory data, HPLC results, and therapeutic blockade information. This material is available free of charge via the Internet at http://pubs.acs.org.

AUTHOR INFORMATION

Corresponding Author

*For S.Y.: phone, +86-10-63165326; fax, 86-10-63017757; e-mail, yushishan@imm.ac.cn. For Z.H.: phone, +86-10-63165207; fax, 86-10-63017757; e-mail, huzhuowei@imm.ac.cn.

Author Contributions

†These authors contributed equally to this work.

Notes

The authors declare no competing financial interest.

ACKNOWLEDGMENTS

This work was financially supported by National Natural Science Foundation of China (Grant No. 201072234, Grant No. 21132009) and the National Science and Technology Project of China (Grant No. 2012ZX09301002-002).

ABBREVIATIONS USED

GL, glycyrrhizin; HMGB1, high-mobility group box 1; LPS, lipopolysaccharide; HF, heart failure; AHF, acute heart failure; CHF, chronic heart failure; RAGE, glycation end products; HBV, hepatitis B virus; DOX, doxorubicin; DCM, Doll Capital Management; PCC, pyridinium chlorochromate; TLR, Toll-like receptor; ip, intraperitoneal; LV, left ventricle; PBS, phosphate buffered saline; PDB, Protein Data Bank; MD, molecular dynamics; THF, tetrahydrofuran; SD, steepest descent; CG, conjugated gradient; GA, genetic algorithm

REFERENCES

(1) Lindenfield, J. Excutive summary: 2010 HFSA comprehensive practice guideline. *J. Card. Failure* **2010**, *16*, 475−539.

(2) Jessup, M.; Abraham, W. T.; Casey, D. E.; Feldman, A. M.; Francis, G. S.; Ganiats, T. G.; Konstam, M. A.; Mancini, D. M.; Rahko, P. S.; Silver, M. A.; Stevenson, L. W.; Yancy, C. W. 2009 focused update: ACCF/AHA guidelines for the diagnosis and management of heart failure in adults: a report of the American College of Cardiology Foundation/American Heart Association Task Force on Practice Guidelines: developed in collaboration with the International Society for Heart and Lung Transplantation. *Circulation* **2009**, *119*, 1977−2016.

(3) McMurray, J. J.; Pfeffer, M. A. Heart failure. *Lancet* **2005**, *365*, 1877−1889.

(4) Lloyd-Jones, D.; Adams, R.; Carnethon, M.; De Simone, G.; Ferguson, T. B.; Flegal, K.; Ford, E.; Furie, K.; Go, A.; Greenlund, K.; Haase, N.; Hailpern, S.; Ho, M.; Howard, V.; Kissela, B.; Kittner, S.; Lackland, D.; Lisabeth, L.; Marelli, A.; McDermott, M.; Meigs, J.; Mozaffarian, D.; Nichol, G.; O'Donnell, C.; Roger, V.; Rosamond, W.; Sacco, R.; Sorlie, P.; Stafford, R.; Steinberger, J.; Thom, T.; Wasserthiel-Smoller, S.; Wong, N.; Wylie-Rosett, J.; Hong, Y. Heart disease and stroke statistics—2009 update: a report from the American Heart Association Statistics Committee and Stroke Statistics Subcommittee. *Circulation* **2009**, *119*, e21−e181.

(5) Jiang, B. B.; Liao, R. The paradoxical role of inflammation in cardiac repair and regeneration. *J. Cardiovasc. Transl. Res.* **2010**, 3, 410−416.

(6) Yang, H.; Wang, H. C.; Czura, C. J.; Tracey, K. J. The cytokine activity of HMGB1. *J. Leukocyte Biol.* **2005**, *78*, 1−8.

(7) Rosenberg, H. F.; Oppenheim, J. J. Interview with Dr. Maurizio C. Capogrossi regarding pivotal advance: high-mobility group box 1 protein—a cytokine with a role in cardiac repair. *J. Leukocyte Biol.* **2007**, *81*, 38−40.

(8) Palumbo, R.; Sampaolesi, M.; De Marchis, F.; Tonlorenzi, R.; Colombetti, S.; Mondino, A.; Cossu, G.; Bianchi, M. E. Extracellular HMGB1, a signal of tissue damage, induces mesoangioblast migration and proliferation. *J. Cell Biol.* **2004**, *164*, 441−449.

(9) Mitola, S.; Belleri, M.; Urbinati., C.; Coltrini, D.; Sparatore, B.; Pedrazzi, M.; Melloni, E.; Presta, M. Cutting edge: extracellular high mobility group box-1 protein is a proangiogenic cytokine. *J. Immunol.* **2006**, *176*, 12−15.

(10) Limana, F.; Gemani, A.; Zacheo, A.; Kajstura, J.; Di Carlo, A.; Borsellino, G.; Leoni, O.; Palumbo, R.; Battistini, L.; Rastaldo, R.; Müller, S.; Pompilio, G.; Anversa, P.; Bianchi, M. E.; Capogrossi, M. C. Exogenous high-mobility group box 1 protein induces myocardial regeneration after infraction via enhanced cardiac C-kit+ cell proliferation and differentiation. *Circ. Res.* **2005**, *97*, e73−e83.

(11) Germani, A.; Limana, F.; Capogrossi, M. C. Pivotal advances: high-mobility group box 1 protein—a cytokine with a role in cardiac repair. *J. Leukocyte Biol.* **2007**, *81*, 41−45.

(12) Li, W.; Sama, A. E.; Wang, H. C. Role of HMGB1 in cardiovascular diseases. *Curr. Opin. Pharmacol.* **2006**, *6*, 130−135.

(13) Li, J.; Kokkola, R.; Tabibzadeh, S.; Yang, R.; Ochani, M.; Qiang, X.; Harris, H. H.; Czura, C. J.; Wang, H. C.; Ulloa, L.; Wang, H.; Warren, H. S.; Moldawer, L. L.; Fink, M. P.; Andersson, U.; Tracey, K. J.; Yang, H. Structure basis for the proinflammatory cytokine activity of high mobility group box 1. *Mol. Med.* **2003**, *9*, 37−45.

(14) Yang, H.; Ochani, M.; Li, J.; Qiang, X.; Tanovic, M.; Harris, H. E.; Susarla, S. M.; Ulloa, L.; Wang, H.; DiRaimo, R.; Czura, C. J.; Wang, H.; Roth, J.; Warren, H. S.; Fink, M. P.; Fenton, M. J.; Andersson, U.; Tracey, K. J. Reversing established sepsis with antagonists of endogenous high-mobility group box1. *Proc. Natl. Acad. Sci. U.S.A.* **2004**, *101*, 296−301.

(15) Dumitriu, I. E.; Baruah, P.; Manfredi, A. A.; Bianchi, M. E.; Rovere-Querini, P. HMGB1: guiding immunity from within. *Trends. Immunol.* **2005**, *26*, 381−387.

(16) Andrassy, M.; Volz, H. C.; Igwe, J. C.; Funke, B.; Eichberger, S. N.; Kaya, Z.; Buss, S.; Autschbach, F.; Pleger, S. T.; Lukic, I. K.; Bea, F.; Hardt, S. E.; Humpert, P. M.; Bianchi, M. E.; Mairbäurl, H.; Nawroth, P. P.; Remppis, A.; Katus, H. A.; Bierhaus, A. High-mobility group box-1 in ischemia−reperfusion injury of the heart. *Circulation* **2008**, *117*, 3216−3226.

(17) Takahashi, K.; Fukushima, S.; Yamahara, K.; Yashiro, K.; Shintani, Y.; Coppen, S. R.; Salem, H. K.; Brouilette, S. W.; Yacoub, M. H.; Suzuki, Ken. Modulated inflammation by injection of high-mobility group box 1 recovers post-infarction chronically failing heart. *Circulation* **2008**, *118*, S106−S114.

(18) (a) Newman, D. J.; Cragg, G. M.; Snader, K. M. The influence of natural products upon drug discovery. *Nat. Prod. Rep.* **2000**, *17*, 215−234. (b) Newman, D. J.; Cragg, G. M.; Snader, K. M. Natural products as sources of new drugs over the period 1981−2002. *J. Nat. Prod.* **2003**, *66*, 1022−1037. (c) Newman, D. J.; Cragg, G. M. Natural products as sources of new drugs over the last 25 years. *J. Nat. Prod.* **2007**, *70*, 461−477. (d) Newman, D. J.; Cragg, G. M. Natural products as sources of new drugs over the 30 years from 1981−2010. *J. Nat. Prod.* **2012**, *75*, 311−335.

(19) Mollica, L.; Marchis, F. D.; Spitaleri, A.; Dallacosta, C.; Pennacchini, D.; Zamai, M.; Agresti, A.; Trisciuoglio, L.; Musco, G.; Bianchi, M. E. Glycyrrhizin binds to high-mobility group box 1 protein and inhibits its cytokine activities. *Chem. Biol.* **2007**, *14*, 431−441.

(20) Sitia, G.; Lannacone, M.; Müller, S.; Bianchi, M. E.; Guidotti, L. G. Treatment with HMGB1 inhibitors diminishes CTL-induced liver disease in HBV transgenic mice. *J. Leukocyte Biol.* **2007**, *81*, 100−107.

(21) Baltina, L. A. Chemical modification of glycyrrhizic acid as a route to new bioactive compounds for medicine. *Curr. Med. Chem.* **2003**, *10*, 155−171.

(22) Hirabayashi, K.; Iwata, S.; Matsumoto, H.; Mori, T.; Shibata, S.; Bara, M.; Ito, M.; Shigeta, S.; Nakashima, H.; Yamamoto, N. Antiviral activities of glycyrrhizin and its modified compounds against human immunodeficiency virus type 1 (HIV-1) and herpes simplex virus type 1 (HSV-1) in vitro. *Chem. Pharm. Bull.* **1991**, *39*, 112−115.

(23) Hardman, C. H.; Broadhurst, R. W.; Raine, A. R.; Grasser, K. D.; Thomas, J. O.; Laue, E. D. Structure of the A-domain of HMG1 and its interaction with DNA as studied by heteronuclear three- and four-dimensional NMR spectroscopy. *Biochemistry* **1995**, *34*, 16596−16607.

(24) Weir, H. M.; Kraulis, P. J.; Hill, C. S.; Raine, A. R.; Laue, E. D.; Thomas, J. O. Structure of the HMG box motif in the B-domain of HMG1. *EMBO J.* **1993**, *12*, 1311−1319.
(25) Jones, G. Development and validation of a genetic algorithm for flexible docking. *J. Mol. Biol.* **1997**, *267*, 727−748.
(26) Berendsen, H. J. C.; van der Spoel, D.; van Drunen, R. GROMACS: a message-passing parallel molecular dynamics implementation. *Comput. Phys. Commun.* **1995**, *91*, 43−56.
(27) Sasaki, Y.; Mizutani, K.; Kasai, R.; Tanaka, O. Solubilizing properties of glycyrrhizin and its derivatives: solubilization of saikosaponin-a, the saponin of Bupleuri Radix. *Chem. Pharm. Bull.* **1988**, *36*, 3491−3495.
(28) Östberg, T.; Wähämaa, H.; Palmblad, K.; Ito, N.; Stridh, P.; Shoshan, M.; Lotze, M. T.; Harris, H. E.; Andersson, U. Oxaliplatin retains HMGB1 intranuclearly and ameliorates collagen type II-induced arthritis. *Arthritis Res. Ther.* **2008**, *10*, R1−R9.
(29) Yang, H.; Hreggvidsdottir, H. S.; Palmblad, K.; Wang, H. C.; Ochani, M.; Li, J. H.; Lu, B.; Chavan, S.; Rosas-Ballina, M.; Al-Abed, Y.; Akira, S.; Bierhaus, A.; Erlandsson-Harris, H.; Andersson, U.; Tracey, K. J. A critical cysteine is required for HMGB1 binding to Toll-like receptor 4 and activation of macrophage cytokine release. *Proc. Natl. Acad. Sci. U.S.A.* **2010**, *107*, 11942−11947.
(30) Liu, Y. Y.; Cai, W. F.; Yang, H. Z.; Cui, B.; Chen, Z. H; Liu, H. Z.; Yan, J.; Jin, W.; Yan, H. M.; Xin, B. M.; Yuan, B.; Hua, F.; Hu, Z. W. Bacillus calmette-guérin and TLR4 agonist prevent cardiovascular hypertrophy and fibrosis by regulating immune microenviroment. *J. Immunol.* **2008**, *180*, 7349−7357.
(31) Cai, W. F.; Zhang, X. W.; Yan, H. M.; Ma, Y. G.; Wang, X. X.; Yan, J.; Xin, B. M.; Lv, X. X.; Wang, Q. Q.; Wang, Z. Y.; Yang, H. Z.; Hu, Z. W. Intracellular or extracellular heat shock protein 70 differentially regulates cardiac remodeling in pressure overload mice. *Cardiovasc. Res.* **2010**, *88*, 140−149.
(32) Weiner, S. J; Kollman, P. A.; Case, D. A.; Singh, U. C.; Ghio, C.; Alagona, G.; Profeta, S.; Weiner, P. K. A new force field for molecular mechanical simulation of nucleic acids and proteins. *J. Am. Chem. Soc.* **1984**, *106*, 765−784.
(33) Clark, M.; Cramer, R. D.; Van, O. N. Validation of the general purpose Tripos 5.2 force field. *J. Comput. Chem.* **1989**, *10*, 982−1012.